

Current status of the problem of thermal Casimir forceG. L. Klimchitskaya^{1,2} and V. M. Mostepanenko^{1,2,3}¹*Central Astronomical Observatory at Pulkovo of the Russian Academy of Sciences,
Saint Petersburg, 196140, Russia*²*Peter the Great**Saint Petersburg Polytechnic University, Saint Petersburg, 195251, Russia*³*Kazan Federal University, Kazan, 420008, Russia**g.klimchitskaya@mail.ru, vmostepa@gmail.com*

Received 16 December 2021

Accepted 11 January 2022

The problem of thermal Casimir force, which consists in disagreement of theoretical predictions of the fundamental Lifshitz theory with the measurement data of high precision experiments and some peculiar properties of the Casimir entropy, is reviewed. We discuss different approaches to the resolution of this problem proposed in the literature during the last twenty years. Particular attention is given to the role of the effects of spatial dispersion. The recently suggested nonlocal Drude-like permittivities which take proper account of the dissipation of conduction electrons and bring the predictions of the Lifshitz theory in agreement with experiment and requirements of thermodynamics are considered. The prospects of this approach in the ultimate resolution of the problem of thermal Casimir force are evaluated.

Keywords: Thermal Casimir force; Lifshitz theory; high precision experiments; spatial dispersion; Casimir entropy; Nernst heat theorem.

PACS Nos.: 12.20.Fv; 12.20.Ds

1. Introduction

At zero temperature the Casimir force per unit area of two parallel ideal metal plates spaced at a distance a (i.e., the Casimir pressure) is expressed¹ as $-\pi^2\hbar c/(240a^4)$. This force originates from the zero-point fluctuations of quantized electromagnetic field whose spectra in the presence of planes and in the free space are different. At nonzero temperature of ideal metal planes, $T \neq 0$, the Casimir pressure was investigated in several papers.²⁻⁴ At low ($T \ll T_{\text{eff}}$) and high ($T \gg T_{\text{eff}}$) temperature, where $k_B T_{\text{eff}} \equiv \hbar c/(2a)$, it is given by

$$P(a, T) = -\frac{\pi^2\hbar c}{240a^4} \left[1 + \frac{1}{3} \left(\frac{T}{T_{\text{eff}}} \right)^4 \right], \quad P(a, T) = -\frac{k_B T}{4\pi a^3} \zeta(3), \quad (1)$$

respectively, where k_B is the Boltzmann constant and $\zeta(3)$ is the Riemann zeta function. These results are determined by the zero-point and thermal fluctuations

2 *G. L. Klimchitskaya & V. M. Mostepanenko*

of the electromagnetic field. They are quite reasonable. Specifically, the respective Casimir entropy per unit area of ideal metal planes goes to zero with vanishing temperature in line with the Nernst heat theorem.⁵

The Casimir result obtained for ideal metal planes was generalized by Lifshitz⁶ for the case of two parallel thick plates (semispaces) at temperature T described by the frequency-dependent dielectric permittivity which plays a role of the response function to electromagnetic fluctuations. At a later time, the Lifshitz theory was generalized⁷ for magnetic materials described by the magnetic permeability. An application region of the Lifshitz theory is restricted by the fact that it treats the plate material classically using the continuous permittivity and permeability functions. Furthermore, the original formulation of this theory takes no account of the spatial dispersion.

Lifshitz derived his theory on the basis of the fluctuation-dissipation theorem of quantum statistical physics. This approach is only applicable to the boundary plates made of usual materials possessing the dissipation properties. The respective response functions should be complex, i.e., have some nonzero pure imaginary parts in order the obtained expressions for the force be nonzero. The reverse is, however, incorrect. If one substitutes the real dielectric function into the Lifshitz formula, the obtained Casimir force is not equal to zero.

Another approach to the derivation of the Lifshitz theory is based on quantum field theory with appropriate boundary conditions. In doing so, the boundary conditions used by Casimir (the tangential component of electric field and the normal component of magnetic induction vanish on the ideal metal planes) are replaced by the standard continuity conditions of classical electrodynamics. The resulting formula for the force coincides with the Lifshitz formula under an assumption of real dielectric permittivity and permeability functions.^{8–10} This assumption is needed for obtaining real energy eigenvalues of the problem. A generalization of the quantum field theoretical approach to the case of dissipative materials is reached by considering some auxiliary electrodynamic problem.¹¹

Note that the two above approaches are somewhat complementary. The first of them faces problems for the case of ideal metal planes (specifically, the Casimir result follows from the Lifshitz formula by using the special prescription¹²). The fluctuation-dissipation approach is also inapplicable to calculation of the Casimir energies in some problems of elementary particle physics (e.g., in the bag model of hadrons^{13,14}) and in cosmological models with nontrivial topology (where the boundary conditions are replaced with the identification conditions^{15–17}). On the other case, as mentioned above, the second, field-theoretical, approach encounters difficulties and should be supplemented when applied to the configurations with boundary bodies made of usual, dissipative, materials. Allowance must be also made to the fact that in the most of cases the dielectric functions of condensed matter physics are of more or less phenomenological character and this may plague an application of the Lifshitz theory to some specific systems and a comparison between the measurement data and theoretical predictions.

In this review, we consider the current status of the problem of thermal Casimir force which was actively discussed in the literature for the last twenty years. The point is that for usual metals described by the Drude model the Lifshitz theory predicts an unexpectedly big thermal correction at short separations between the plates which decreases the magnitude of attractive (negative) Casimir force.¹⁸ This problem is not resolved yet because theoretical predictions of the Lifshitz theory for the room-temperature Casimir force calculated using the Drude model and similar response functions for both metallic and dielectric materials turned out to be in conflict with the measurement data of high precision experiments performed by different experimental groups. However, the main facts in this field of research are by now established and some ways to the resolution of the problem are directed.

The structure of the review is as follows. In Sec. 2, an essence of the problem of thermal Casimir force between both metallic and dielectric test bodies is elucidated. Section 3 presents what is known from the high precision experiments on measuring the Casimir interaction. In Sec. 4, different theoretical approaches to the resolution of this problem proposed during the last years are briefly considered. Section 5 is devoted to the question on whether an alternative response to the evanescent waves could solve the problem. Finally, Sec. 6 contains our conclusions and outlook.

2. Problem of the Thermal Correction to the Casimir Force

The Lifshitz theory expresses the Casimir force per unit area of material plates (i.e., the Casimir pressure P) as a functional of their dielectric permittivity $\varepsilon(\omega)$ and magnetic permeability $\mu(\omega)$ which depend on frequency ω and may also depend on T . For the case of two similar plates the result is^{6,17}

$$P(a, T) = -\frac{\hbar}{2\pi^2} \int_0^\infty k_\perp dk_\perp \int_0^\infty d\omega \coth \frac{\hbar\omega}{2k_B T} \times \text{Im} \left\{ q [r_{\text{TM}}^{-2}(\omega, k_\perp) e^{2aq} - 1]^{-1} + q [r_{\text{TE}}^{-2}(\omega, k_\perp) e^{2aq} - 1]^{-1} \right\}, \quad (2)$$

where $k_\perp = (k_1^2 + k_2^2)^{1/2}$ is the magnitude of the wave vector projection on a plane of the plates and $q \equiv q(\omega, k_\perp) = (k_\perp^2 - \omega^2/c^2)^{1/2}$. The transverse magnetic (TM) and transverse electric (TE) reflection coefficients are defined as

$$r_{\text{TM}}(\omega, k_\perp) = \frac{\varepsilon(\omega)q - k(\omega, k_\perp)}{\varepsilon(\omega)q + k(\omega, k_\perp)}, \quad r_{\text{TE}}(\omega, k_\perp) = \frac{\mu(\omega)q - k(\omega, k_\perp)}{\mu(\omega)q + k(\omega, k_\perp)} \quad (3)$$

and

$$k(\omega, k_\perp) = \left[k_\perp^2 - \varepsilon(\omega)\mu(\omega)\frac{\omega^2}{c^2} \right]^{1/2}. \quad (4)$$

It is seen that (2) can be represented as the contributions of propagating waves for which $\omega > ck_\perp$ and evanescent waves with $0 \leq \omega \leq ck_\perp$. The propagating waves satisfy the mass-shell equation in free space. The evanescent waves are off the mass shell (one can say that they are characterized by the pure imaginary k_3).

4 *G. L. Klimchitskaya & V. M. Mostepanenko*

Taking into account that the contribution of propagating waves in (2) contains the rapidly oscillating functions due to the pure imaginary q (but real k_3), in computations it is more convenient to use the mathematically equivalent representation for $P(a, T)$ in terms of the pure imaginary Matsubara frequencies^{6,17}

$$P(a, T) = -\frac{k_B T}{\pi} \sum_{l=0}^{\infty}{}' \int_0^{\infty} q_l k_{\perp} dk_{\perp} \left\{ [r_{\text{TM}}^{-2}(i\xi_l, k_{\perp}) e^{2aq_l} - 1]^{-1} + [r_{\text{TE}}^{-2}(i\xi_l, k_{\perp}) e^{2aq_l} - 1]^{-1} \right\}. \quad (5)$$

Here, the Matsubara frequencies are $\xi_l = 2\pi k_B T l / \hbar$ with $l = 0, 1, 2, \dots$, the prime on the summation sign divides the term with $l = 0$ by two, and q_l is obtained from q by putting $\omega = i\xi_l$.

The thermal correction to the zero-temperature Casimir pressure is defined as

$$\Delta_T P(a, T) = P(a, T) - P(a, 0). \quad (6)$$

We consider it separately for metallic and dielectric plates.

2.1. *Thermal correction to the Casimir force between metallic plates*

To calculate the Casimir force and the thermal correction to it one needs to know the response functions of a metal within sufficiently wide frequency region. In measurements of the Casimir force the nonmagnetic metal Au is in most common use. The optical data for the complex index of refraction of Au were measured¹⁹ over the range of frequencies from $\hbar\omega = 0.125$ eV to $\hbar\omega = 10^4$ eV making available both real and imaginary parts of the dielectric permittivity of Au, $\text{Re } \varepsilon_{\text{opt}}$ and $\text{Im } \varepsilon_{\text{opt}}$, in the same frequency range.

It should be especially emphasized that the dielectric response is measured in optical experiments exploiting the propagating waves. It is an assumption that the same response can be used in the area of evanescent waves as well.

To determine $\varepsilon(i\xi)$ along the imaginary frequency axis, as required in (5), it is necessary to extrapolate the measured $\text{Im } \varepsilon_{\text{opt}}$ to zero frequency and apply the Kramers-Kronig relation.¹⁷ Under an assumption that the effects of spatial dispersion are sufficiently small (this is certainly true for the propagating waves), the Maxwell equations result in the first expansion term of ε at low frequencies, $\varepsilon(\omega) = i4\pi\sigma_0/\omega$, where σ_0 is the conductivity at constant current.²⁰ This term is well reproduced by the Drude model²¹

$$\varepsilon_D(\omega) = 1 - \frac{\omega_p^2}{\omega[\omega + i\gamma(T)]}, \quad (7)$$

where ω_p is the plasma frequency, $\gamma(T)$ is the relaxation parameter and $\sigma_0 = \omega_p^2/(4\pi\gamma)$. The imaginary part of (7) is commonly used for an extrapolation of the optical data for $\text{Im } \varepsilon_{\text{opt}}(\omega)$ to $\omega = 0$. It was found^{19,22} that for Au $\hbar\omega_p = 9.0$ eV and $\hbar\gamma(300 \text{ K}) = 0.035$ eV.

However, as mentioned in Sec. 1, the Lifshitz theory using the permittivity (7) predicts rather big thermal correction to the Casimir force which decreases the force magnitude.¹⁸ In Fig. 1 the relative thermal correction $\delta_T P(a, T) = \Delta_T P(a, T)/P(a, 0)$ computed by (3) and (5)–(7) at $T = 300$ K is shown by the bottom line as a function of separation between the plates (note that the use of optical data at $\hbar\omega \geq 0.125$ eV makes only a minor impact on the computational results and only at $a < 0.5$ μm). As can be seen in Fig. 1, this correction reaches -6.4% , -9.4% , and -13.8% at $a = 0.5$, 0.7 , and 1 μm , respectively, and vanishes at $a = 6.3$ μm .

The results for Au plates should be compared with respective results for the ideal metal planes (1). Thus, from the first equality in (1) one obtains that for ideal metal planes the relative thermal correction takes the positive values, is equal to only 0.0098% and 0.157% at $a = 0.5$ and 1 μm , respectively, and increases with increasing separation. At large separations (high temperatures) for Au plates described by the Drude model, one obtains one half of the result given by the second equality in (1) for ideal metal planes.

So strong discrepancy between the thermal corrections predicted theoretically for the plates made of a good metal and for the ideal metal planes may look incredible. Taking into account that for two plates spaced at a distance a of the order of micrometer the characteristic frequency c/a belongs to the region of infrared optics, it has long been usable to calculate the Casimir force employing the dielectric permittivity of dissipationless plasma model^{12, 23, 24}

$$\varepsilon_p(\omega) = 1 - \frac{\omega_p^2}{\omega^2}, \quad (8)$$

which is obtained from (7) by putting $\gamma(T) = 0$.

In Fig. 1, the relative thermal correction calculated by (3), (5), (6), and (8) is shown by the top line. Although an application of (8) at low frequencies including the zero frequency is physically unjustified, the thermal correction shown by the top

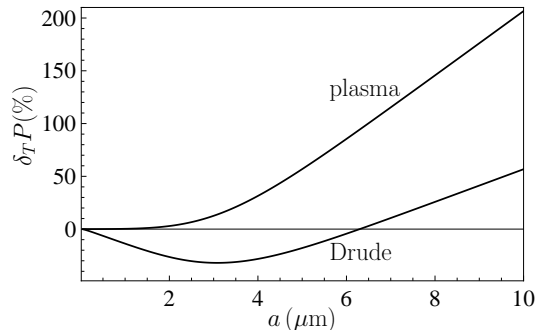


Fig. 1. The relative thermal correction to the Casimir pressure between Au plates computed at $T = 300$ K using the Drude and plasma models is shown as a function of separation by the bottom and top lines, respectively.

6 *G. L. Klimchitskaya & V. M. Mostepanenko*

line demonstrates the same characteristic properties as in the case of ideal metal planes, i.e., it is positive, small at short separations and increases monotonously with increasing separation. Specifically, at $a = 0.5$ and $1 \mu\text{m}$ the relative thermal correction shown by the top line is equal to 0.058% and 0.29%, respectively. In the high temperature limit, the thermal Casimir force calculated using the plasma model is given by the second equality in (1) found in the case of ideal metal planes.

One more fact that deserves attention is regarding an agreement between the Lifshitz theory and thermodynamics. It was shown that for metals with perfect crystal lattice, which is the basic idealization of condensed matter physics, the Casimir entropy calculated using the Drude model (7) violates the third law of thermodynamics (the Nernst heat theorem) by taking a nonzero (negative) value at $T = 0$ depending on the parameters of a system.^{25–28} If, however, the plasma model (8) is used, the Lifshitz theory results in the zero Casimir entropy at $T = 0$, i.e., the Nernst heat theorem is satisfied.^{25–28} It is necessary to stress that in reality metallic crystal lattices contain some fraction of impurities leading to small nonzero relaxation at zero temperature $\gamma(0) = \gamma_0$ (for a perfect crystal lattices $\gamma_0 = 0$). In this case it was shown that the Casimir entropy jumps to zero at small T starting from the negative values, i.e., the validity of the Nernst heat theorem is restored.^{29–31}

2.2. Thermal correction to the Casimir force between dielectric plates

As opposite to metals, the dielectric materials possess the zero electric conductivity at $T = 0$. The optical data for dielectric materials, similar to the case of metals, can be measured over the wide frequency region¹⁹ and are basically independent on T . This gives the possibility to obtain their frequency-dependent dielectric permittivity $\varepsilon_{\text{opt}}(\omega)$. In reality, however, dielectric materials possess some nonzero conductivity $\sigma_0(T)$ at any nonzero temperature which decreases with vanishing T exponentially fast. As a result, the permittivity function of dielectric materials takes the form¹⁹

$$\varepsilon(\omega) = \varepsilon_{\text{opt}}(\omega) + i \frac{4\pi\sigma_0(T)}{\omega}. \quad (9)$$

Similar to the metals described by the Drude model, the Casimir force between two dielectric plates described by the permittivity (9) demonstrates an unexpectedly big thermal effect at short separations. As an example, in Fig. 2 the relative thermal correction to the Casimir pressure between two fused silica plates computed by (3), (5) and (9) is shown by the top line as a function of separation at $T = 300$ K. In computations, the values $\varepsilon_{\text{opt}}(0) = 3.81$ and $\sigma_0 = 29.7 \text{ s}^{-1}$ have been used¹⁹ (note that these results are independent on a specific value of σ_0 , but only on the fact that it is nonzero). According to Fig. 2, at separations of 1 and 2 μm the relative thermal correction is equal to 182% and 314%, respectively. In the high temperature limit, the thermal Casimir force between dielectric plates described by (9) is equal to one half of the result for ideal metals given by the second equality in (1) similar to the case of metals described by the Drude model (7).

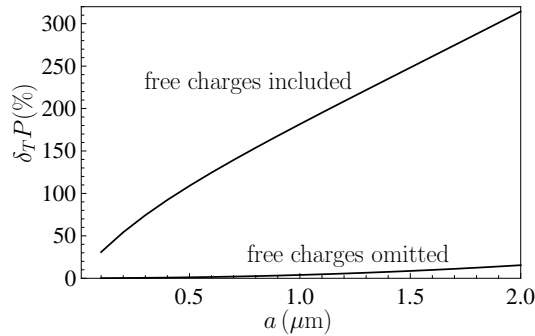


Fig. 2. The relative thermal correction to the Casimir pressure between fused silica plates computed at $T = 300$ K with included and omitted free charge carriers is shown as a function of separation by the top and bottom lines, respectively.

Taking into account that the conductivity of dielectric materials is a very small effect, it was often omitted in calculations.^{32–36} In this case the dielectric properties of the plates were characterized by $\varepsilon_{\text{opt}}(\omega)$. The computational results for the relative thermal correction to the Casimir pressure between two fused silica plates described by $\varepsilon_{\text{opt}}(\omega)$ are shown by the bottom line in Fig. 2 as a function of separation at $T = 300$ K. For the plates spaced at 1 and 2 μm the relative thermal correction is equal to only 3.9% and 15.4%, respectively, i.e., much fewer than with included conductivity. In the limit of high temperature, the Casimir pressure calculated with omitted conductivity is given by¹⁷

$$P(a, T) = -\frac{k_B T}{8\pi a^3} \text{Li}_3 \left[\left(\frac{\varepsilon_0 - 1}{\varepsilon_0 + 1} \right)^2 \right], \quad (10)$$

where $\text{Li}_n(z)$ is a polylogarithm function.

What is more, the use of the dielectric permittivity (9) with included conductivity of a dielectric material at $T \neq 0$ results in violation of the Nernst heat theorem.^{37–42} In this case the Casimir entropy at $T = 0$ is positive and again depends on the system parameters. However, if one describes the dielectric materials by $\varepsilon_{\text{opt}}(\omega)$, the Nernst heat theorem is satisfied.^{37–42} The Lifshitz theory using the permittivity (9) can be reconciled with the Nernst heat theorem by assuming that dielectric materials possess some nonzero conductivity down to zero temperature.⁴³ This is, however, not the case of real dielectrics.

3. What is Known from High Precision Experiments

Several high precision experiments on measuring the Casimir interaction in sphere-plate geometry have been performed by Ricardo Decca using a micromechanical torsional oscillator and by Umar Mohideen by means of a modified atomic force microscope (AFM). All these experiments were done in high vacuum, benefited from direct measurements of the force-distance relations, and took an advantage of

rigorous procedures for comparison between experiment and theory with no fitting parameters. In this connection, the experiment on measuring the Casimir force between a spherical lens of centimeter-size curvature radius and a plate performed by means of the torsion pendulum⁴⁴ does not fall into the category of high-precision measurements because a comparison between the measurement data and theory was made with two fitting parameters.

3.1. Measurements by means of a micromechanical torsional oscillator

In three subsequent experiments, the gradient of the Casimir force between an Au-coated sphere of radius R and an Au-coated plate $F'_{sp}(a, T)$ was measured by means of a micromechanical torsional oscillator^{45–48} and recalculated into the effective Casimir pressure between two plane parallel plates using the proximity force approximation (PFA)

$$P(a, T) = -\frac{1}{2\pi R} F'_{sp}(a, T). \quad (11)$$

The roughness on the surfaces of both test bodies was measured by means of an atomic force microscope and taken into account perturbatively.^{49,50} In Fig. 3 we show two representative examples⁴⁷ of the comparison between experiment and theory where the bottom and top theoretical bands for the effective pressure are computed at $T = 300$ K by (3), (5), and the optical data for Au extrapolated down to zero frequency using the plasma model (8) and the Drude model (7), respectively. The experimental data are shown as crosses with their total errors determined at the 95% confidence level. It is seen that the theoretical predictions using the plasma model extrapolation (8) are in a good agreement with the data whereas the Drude extrapolation (7) is experimentally excluded.

According to Fig. 3, the difference between two alternative theoretical predictions using different extrapolations reaches only a few percent of the Casimir pres-

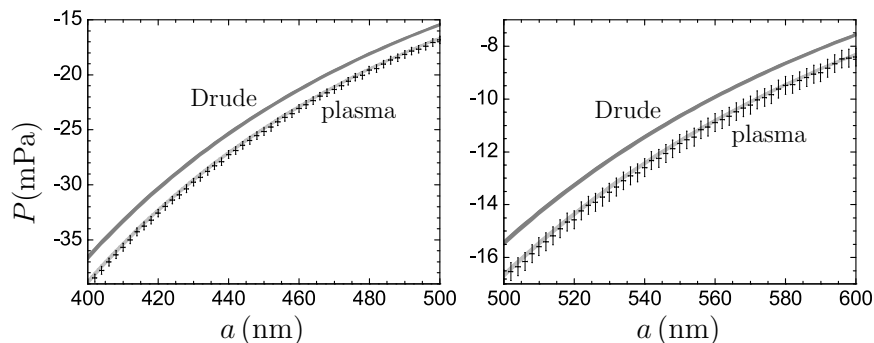


Fig. 3. The effective Casimir pressure between two Au-coated plates computed at $T = 300$ K using either the plasma or Drude extrapolation of the optical data is shown as a function of separation by the bottom and top bands, respectively, over the intervals from 400 to 500 nm (left) and from 500 to 600 nm (right). The measurement data are shown as crosses.

sure magnitude. This difference, however, can be increased significantly by measuring the differential Casimir force.^{51,52} Using this idea, measurements of the differential Casimir force between a Ni-coated sphere and Au and Ni sectors of the disc coated with an Au overlayer have been performed by means of a micromechanical torsional oscillator.⁵³ In the configuration of this experiment, the theoretical predictions using the plasma and Drude extrapolations differ from one another by up to a factor of 1000. As a result, the predictions of the Lifshitz theory using the plasma model extrapolation were found to be in a good agreement with the measurement data whereas the alternative predictions using an extrapolation of the optical data by means of the Drude model were conclusively excluded.

The next experiment was performed recently within a wider range of separations from 0.2 to 8 μm . In this case the micromechanical torsional oscillator was used to measure the differential Casimir force between an Au-coated sphere and the top and bottom of Au-coated deep Si trenches.⁵⁴ An employment of the differential measurement scheme gave the possibility to significantly decrease the total experimental errors (to below 3 fN at separations exceeding 1 μm). Due to the large deepness of the trenches, the force between a sphere and their bottom vanishes. As a result, it is the Casimir force between a sphere and a plane trench top which is measured. This work also differs from the discussed above experiments in that it includes the characterization of patch potentials by means of Kelvin probe microscopy and performs computations of the Casimir force in the sphere-plate geometry based on the recently developed first-principle methods using the scattering theory^{55–58} and the gradient expansion.^{59–62}

In Fig. 4 we present the comparison between experiment and theory over the separation region from 1 to 8 μm which is not covered in previous precision experiments.⁵⁴ The bottom and top solid lines are computed by the exact theory using the plasma and Drude extrapolations of optical data, respectively. The theoretical predictions obtained using the PFA are indicated by the dashed lines. They are not discriminated from the solid lines in the limits of total experimental errors shown as

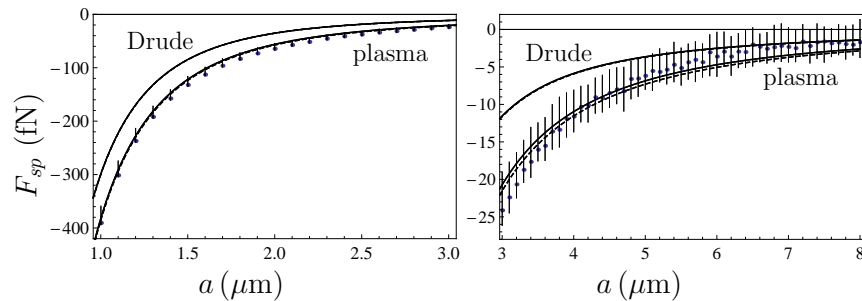


Fig. 4. The Casimir force between an Au-coated sphere and an Au-coated plate computed at $T = 300$ K by the exact theory using either the plasma or Drude extrapolation of the optical data is shown as a function of separation by the bottom and top solid lines, respectively, over the intervals from 1 to 3 μm (left) and from 3 to 8 μm (right). The respective PFA results are presented by the dashed lines. The measurement data are shown as crosses.

crosses which are determined at the 95% confidence level. As can be seen in Fig. 4, the theoretical predictions using the extrapolation by means of the Drude model are experimentally excluded over the separation region $a < 4.8 \mu\text{m}$. The predictions obtained with the help of the plasma model extrapolation of the optical data are in agreement with the data over the entire measurement range.

It is significant that the difference between two alternative theoretical predictions in Figs. 3 and 4 is entirely caused by the respective difference in thermal corrections in Fig. 1 using the Drude and plasma extrapolations of the optical data to zero frequency.

3.2. Measurements by means of an atomic force microscope

In four experiments, the gradient of the Casimir force between an Au-coated sphere and an Au-coated plate $F'_{sp}(a, T)$ was measured using a modified AFM operated in the dynamic mode.^{63–66} Similar measurements were also performed^{67–69} in configurations where either a plate or both a sphere and a plate were coated with a magnetic (but not magnetized) metal Ni. Using the PFA, the gradient of the Casimir force F'_{sp} was expressed via the Casimir pressure for two parallel plates (2) or (5) found in the framework of the Lifshitz theory

$$F'_{sp}(a, T) = -2\pi RP(a, T). \quad (12)$$

Small corrections to (12) due to surface roughness and deviations from PFA were taken into account perturbatively and contributed only a fraction of percent. Much care was taken to diminish the role of electrostatic effects arising due to the residual potentials and surface patches. Specifically, the setups of three experiments^{64–66} were equipped with an Ar-ion guns and UV lamps allowing to perform additional cleaning procedures of the sphere and plate surfaces.

In Fig. 5, the typical results for the gradients of the Casimir force between Au-coated test bodies measured in this way are shown as crosses where the total experimental errors are determined at the 67% confidence level.⁶⁶ The bottom and

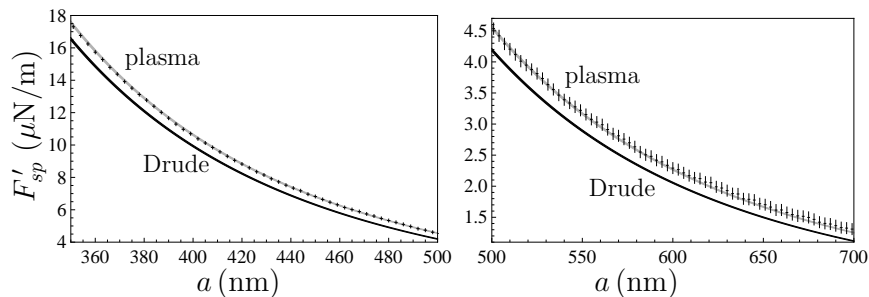


Fig. 5. The gradient of the Casimir force between an Au-coated sphere and an Au-coated plate computed at $T = 300\text{K}$ using either the Drude or plasma extrapolation of the optical data is shown as a function of separation by the bottom and top bands, respectively, over the intervals from 350 to 500 nm (left) and from 500 to 700 nm (right). The measurement data are shown as crosses.

top theoretical bands are computed by (3), (5), and (12) where the optical data for Au were extrapolated using the Drude and plasma models, respectively. It is again seen that the Lifshitz theory using the plasma model extrapolation agrees with the measurement data whereas the same theory using the Drude model extrapolation is excluded by the data.

An application of the atomic force microscope setup to the first measurements of the Casimir interaction with magnetic test bodies^{67–69} was especially important for the problem of thermal Casimir force. The reason is that for an Au-coated sphere above a Ni-coated plate at the experimental separations of several hundred nanometers the Lifshitz theory using the Drude and plasma extrapolations of the optical data leads to almost coinciding theoretical predictions for the force gradients.⁶⁷ As to the case of both test bodies coated with the magnetic metal Ni, the force gradients computed using the plasma model extrapolation turned out to be smaller than those computed using the Drude model.^{68,69} This is on the contrary to the case of two nonmagnetic metals (see Fig. 5).

Figure 6 (left) demonstrates the force gradients measured in the experiment⁶⁷ between an Au-coated sphere and a Ni-coated plate. They are shown as crosses where the total experimental errors were determined at the 67% confidence level. These data are in good agreement with the theoretical band which indicates the joint predictions obtained with either the Drude or the plasma model extrapolation. In Fig. 6 (right), the measured force gradients between a Ni-coated sphere and a Ni-coated plate are presented as crosses. These data are in a good agreement with the bottom theoretical band computed using the plasma model extrapolation. The top band computed with the Drude model extrapolation is excluded by the data.

The modified atomic force microscope was also used for testing the thermal Casimir force with dielectric test bodies. Thus, the differential Casimir force F_{diff} between an Au-coated sphere and a Si membrane was measured in the presence and in the absence of laser pulse on this membrane.^{70,71} The membrane was made

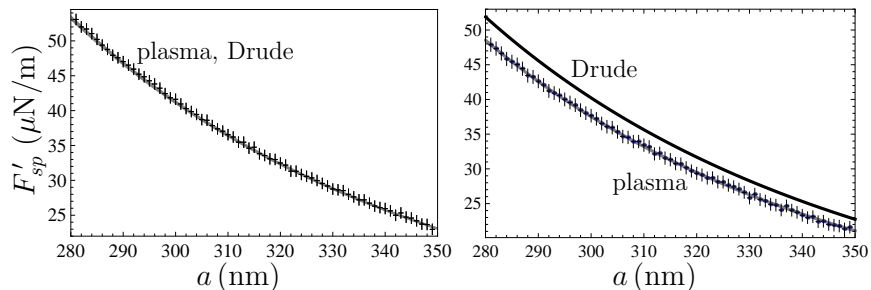


Fig. 6. The gradient of the Casimir force between an Au-coated sphere and a Ni-coated plate computed at $T = 300\text{K}$ using either the Drude or plasma extrapolation of the optical data is shown as a function of separation by the common band (left). For the Ni-coated surfaces of a sphere and a plate, the force gradient computed at $T = 300\text{K}$ using either the plasma or Drude extrapolation is shown by the bottom and top bands, respectively (right). In both cases the measurement data are shown as crosses.

of p -type dielectric Si with the charge carrier concentration of approximately $5 \times 10^{14} \text{ cm}^{-3}$, i.e., much below the critical value at which Si transforms into a metallic state. In the presence of a laser pulse, the concentration of charge carriers jumped to $(1 - 2) \times 10^{19} \text{ cm}^{-3}$, i.e., an illuminated membrane was in the metallic state.

In Fig. 7, the measured difference of the Casimir forces in the presence and in the absence of light is indicated as crosses at different sphere-plate separations where the experimental errors were determined at the 95% confidence level. The bottom and top theoretical lines were computed at $T = 300 \text{ K}$ using the Lifshitz theory and the PFA with the dielectric permittivity of membrane ε_{opt} and ε from (9), respectively, in the dark (dielectric) state. The charge carriers in Au and in a Si membrane in the presence of a laser pulse were described by the Drude model (in this experiment, the use of the plasma model for Au and for Si in the bright state leads to only minor differences which cannot be discriminated in the limits of experimental errors). As can be seen in Fig. 7, the measurement data exclude the theoretical predictions obtained with taken into account conductivity of a membrane in the dielectric state. The same data are in agreement with theoretical predictions found with this conductivity omitted.

Similar results have been obtained from measuring the Casimir force between an Au-coated sphere and an indium tin oxide (ITO) film deposited on a quartz plate before and after the UV irradiation of the film.^{72,73} It was observed that irradiation leads to a significant decrease in the force magnitude measured with no detectable changes in the optical data of the plate. This was interpreted as a phase transition of an ITO film from a metallic to a dielectric state under the influence of UV irradiation. In doing so, the measured Casimir force between an Au-coated sphere and an irradiated film agrees with the theoretical predictions only if the film material is described by the permittivity $\varepsilon_{\text{opt}}(\omega)$ with the role of free charge carriers omitted.^{72,73}

In the end of this section it is necessary to briefly discuss an experiment on

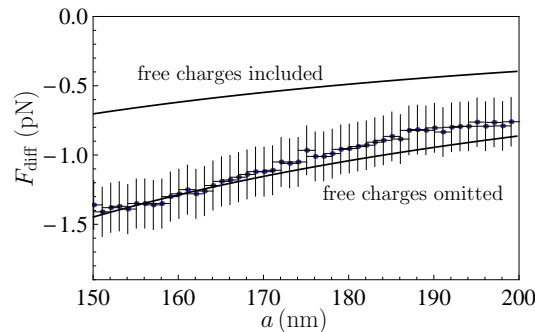


Fig. 7. The differential Casimir force between an Au-coated sphere and a Si membrane in the presence and in the absence of laser pulse on its surface computed at $T = 300 \text{ K}$ with either omitted or included free charge carriers in a membrane in the dark state is shown as a function of separation by the bottom and top lines, respectively. The measurement data are shown as crosses.

measuring the thermal Casimir-Polder force between ^{87}Rb atoms belonging to the Bose-Einstein condensate and a dielectric fused silica plate.³⁶ Although it is not performed by means of an AFM, the obtained results are akin to those found for dielectric materials by means of an AFM. In this experiment, the condensate cloud was resonantly driven into a dipole oscillation by the magnetic field and the shift of the oscillation frequency caused by the Casimir-Polder force was measured over the range of separations from 7 to 11 μm . The measurements were performed both in thermal equilibrium (when the plate temperature $T_p = 310$ K was equal to the environmental temperature) and out of thermal equilibrium conditions ($T_p = 479$ K and $T_p = 645$ K). In the equilibrium conditions, the Casimir-Polder force and respective frequency shift were computed by the Lifshitz theory using the dielectric permittivity $\varepsilon_{\text{opt}}(\omega)$ of fused silica with neglected contribution of nonzero conductivity. The computational results were found to be in a good agreement with the measurement data.³⁶ If, however, computations of the Casimir-Polder force are performed with the permittivity (9) taking into account the conductivity of fused silica, the respective frequency shifts are excluded by the data.⁷⁴

Thus, the measurement data of high precision Casimir experiments with dielectric test bodies agree with theoretical predictions under a condition that the contribution of free charge carriers into the dielectric permittivity is omitted.

4. Theoretical Approaches to the Resolution of the Problem

According to a large body of research presented above, theoretical description of the thermal Casimir force faces with serious difficulties. The Lifshitz theory of the Casimir force using the most realistic response functions taking into account the relaxation properties of conduction electrons in metals and free charge carriers in dielectrics arrives at violation of the Nernst heat theorem for the plates made both of an idealized metal with perfect crystal lattice and of a usual dielectric material (for usual metallic plates the Nernst theorem is satisfied due to the presence of some fraction of impurities).

What is more, the theoretical predictions of the Lifshitz theory using the realistic response functions come into conflict with the measurement data of all high precision experiments performed with both metallic and dielectric test bodies. An agreement between experiment and theory is restored when one neglects by the actually existing phenomena, such as the relaxation of conduction electrons in metals and the presence of free charge carriers in dielectrics at any nonzero temperature. This situation cannot be considered as satisfactory. Below we briefly list the main approaches proposed in the literature to remedy it.

4.1. Validity of approximate methods

Most of the experiments listed above (with exception of only one⁵⁴ performed in 2021) use the PFA in the comparison between experiment and theory. Taking into account that until recently the accuracy of PFA was unknown, it was suggested⁷⁵

that a disagreement between theory using the conventional response functions and the measurement data may be explained by large errors arising from an application of this approximation. Specifically, using the generalization of the Lifshitz theory in the framework of scattering approach, it was found that for an ideal metal sphere above an ideal metal plate the exact results may depart from the PFA ones.⁷⁵

Similar conclusions were made for usual metals⁷⁶ but for rather big values of the ratio $a/R > 0.2$ (in typical experimental conditions it holds $a/R < 0.01$). By now the corrections to PFA in the sphere-plate geometry are found with taken into account real material properties by means of the Drude and plasma extrapolations of the optical data using the scattering theory^{54–58} and the gradient expansion.^{59–62} It was proven that the PFA is well applicable for a comparison between experiment and theory for the sufficiently small ratios of a separation to a sphere radius.

Another approximate method used in the theory-experiment comparison was an additive approach to the surface roughness.^{49,50} As was noted in the literature, the roughness correction should be taken into account when comparing experiment with theory, especially at the shortest separations between the test bodies.^{77,78} Because of this, it is important to determine how accurate would the calculated Casimir force be if the surface roughness is accounted for additively.

This problem was solved within the scattering approach to the Casimir force. According to the results obtained,^{79,80} the additive approach is well applicable under a condition $a \ll \Lambda_c$ where Λ_c is the roughness correlation length. Computations show that for a typical value of $\Lambda_c = 200$ nm the application region of the additive approach is $a < 2\Lambda_c/3 \approx 130$ nm. In this region, the roughness correction may reach a few percent of the force magnitude even for sufficiently smooth test bodies used in the Casimir experiments. Under a condition $a > \Lambda_c$, the additive approach underestimates the contribution of surface roughness to the Casimir force.^{79,80} It turned out, however, that with increasing a the roughness correction decreases much faster than does the main contribution to the force. Because of this, at separations where the additive approach is inapplicable, one can simply neglect by the roughness correction with no impact on the comparison between experiment and theory.

4.2. Analysis of the role of unaccounted effects

It has been known that one difficulty which plagues measurements of the Casimir interaction is an impact of the spatial distribution of electrostatic potentials arising even on the grounded polycrystal surfaces of a sphere and a plate in high vacuum.⁸¹ The presence of these electrostatic effects, which are called the patch potentials, results in the additional attractive force between a sphere and a plate which increases the magnitude of the measured force. Because of this, in the high precision experiments on measuring the Casimir force special measures were undertaken in order to keep the residual potential difference constant.

It was shown⁸² that the presence of sufficiently large patches on the test body surfaces can compensate the differences between top and bottom theoretical bands

in Fig. 3 and, thus, bring the theoretical predictions using the Drude model extrapolation of the optical data in agreement with the measurement results. However, direct measurements of the electrostatic potentials on the test body surfaces by means of Kelvin probe microscopy demonstrated⁸³ that an additional force originating from the surface patches is below 1% of the predicted Casimir force and, thus, is incapable to explain a difference between the top and bottom bands in Fig. 3.

Moreover, the experiments on measuring the Casimir interaction with magnetic test bodies^{67–69} established that the role of patch potentials in high precision experiments performed at separations below $1\mu\text{m}$ is negligibly small. The point is that any marked patch effect would introduce a disagreement between experiment and theory in Fig. 6 (left) where the theoretical predictions obtained using the Drude and plasma model extrapolations are similar.

As to Fig. 6 (right) related to the case of two magnetic test bodies, the presence of any patch effect would only increase a disagreement between the measurement data and theoretical predictions using the Drude model extrapolation. To bring the latter in agreement with the data, one would need some additional repulsive interaction which cannot be provided by the patch effect. Recall also that the role of patch potentials can be diminished significantly by performing the UV- and Ar-ion cleaning of the surfaces.^{64–66} Thus, the problem of thermal Casimir force is not caused by the patch potentials although their contribution should be carefully taken into account in all high precision experiments (especially in those performed at separations exceeding $1\mu\text{m}$).

One more effect that makes an impact on the comparison between experiment and theory is connected with a choice of the optical data of interacting bodies used in computations. Several high precision measurements employed the handbook data¹⁹ of Au in order to calculate the Casimir force. It was noted, however, that the optical properties of Au films vary for each specific sample, depend on the method of deposition and are characterized by different values of the plasma frequency and relaxation parameter.^{84,85} This should influence the Casimir force and, thus, the comparison between experiment and theory.

An analysis of different sets of optical data for Au samples available in the literature led to the conclusion,^{17,50} however, that they bring to even larger departure of the theoretical predictions using the Drude model extrapolation from the measurement results than the handbook data. Furthermore, in several experiments either the Drude parameters or the complete sets of optical data have been measured by means of ellipsometers for the specific samples used.^{47,48,54,72,73} In doing so, the especially measured optical data did not deviate significantly from the handbook ones with no impact on the comparison of experiment and theory. This means that although it is always preferable to measure the optical data of each specific sample in each successive experiment, the use of handbook data¹⁹ cannot leave to qualitatively incorrect conclusions when comparing experiment with theory.

4.3. *The spatial dispersion and screening effects*

Strictly speaking, the Lifshitz theory is applicable to the plate materials possessing the temporal dispersion. The respective dielectric permittivities of plates depend only on the frequency. The spatial dispersion is characterized by the two dielectric permittivities, the transverse one $\varepsilon^{\text{Tr}}(\omega, \mathbf{k})$ and the longitudinal one $\varepsilon^{\text{L}}(\omega, \mathbf{k})$, which describe the response of matter to the electric fields \mathbf{E} perpendicular and parallel to the wave vector \mathbf{k} , respectively.²⁰ Such permittivities can be introduced only under a condition of space homogeneity which is violated by the presence of two parallel plates separated with a gap. However, in the approximation of specular reflection valid for sufficiently smooth test bodies used in the Casimir experiments it is possible to introduce the fictitious homogeneous medium because an electron reflected on the vacuum gap-plate interface is indistinguishable from an electron coming on the source side of this medium. This makes possible^{86,87} to express the reflection coefficients in the Lifshitz formula via the surface impedances and finally via the permittivities ε^{Tr} and ε^{L} (see Sec. 5).

It has been known that for metals a connection between the electric field and the current becomes nonlocal in the region of the anomalous skin effect which extends over the range of frequencies from approximately 10^{12} to 10^{13} rad/s at $T = 300$ K. With decreasing temperature, the left boundary of this region goes down. The spatial dispersion also appears in the screening of static electric field in materials which contain some fraction of free charge carriers. In doing so, the electric field penetrates into the conducting media to a depth of the screening length. The specific expression for this depth depends on whether the density of charge carriers in the plate material goes to zero (dielectrics) or remains nonzero (metals) with vanishing temperature (the Debye-Hückel and Thomas-Fermi screening lengths, respectively⁸⁸). It should be noted that both the anomalous skin effect and the screening effects occur in real electromagnetic fields (the propagating waves including the case of zero frequency).

The spatially nonlocal dielectric permittivities of electron plasma were calculated in the random phase approximation by means of the Boltzmann transport theory.^{89,90} It was shown that the most important difference from the local response function is demonstrated by the longitudinal permittivity $\varepsilon^{\text{L}}(\omega, \mathbf{k})$. The obtained results and similar in spirit approaches were employed to calculate the Casimir and Casimir-Polder forces.^{86,91–93} The Lifshitz theory using the reflection coefficient at zero frequency accounting for the effects of screening was found⁹¹ in agreement with measurements of the Casimir-Polder force at large ^{87}Rb atom-silica plate separations.³⁶ However, an application of similar approach at all Matsubara frequencies⁹² was as yet excluded⁹⁴ by the results of experiment on measuring the differential Casimir force between an Au-coated sphere and a Si membrane illuminated with laser pulses^{70,71} (see Sec. 3.2).

In the case of metallic Casimir plates, an employment of nonlocal dielectric functions describing the anomalous skin effect leads to negligibly small corrections

to the Casimir force computed using the Drude model⁸⁶ which vary from 0.3% to 0.1% when the separation increases from 100 to 300 nm. Calculation of the thermal Casimir pressure between metallic plates with account of screening effects using the Thomas-Fermi length^{92,93} leads to approximately the same results as the spatially local Drude model. In both cases the obtained theoretical predictions are excluded⁹⁴ by the measurement data of many high precision experiments.^{45–48, 53, 54, 63–66}

The consideration of spatial dispersion allowed to make some progress regarding a violation of the Nernst heat theorem (see Sec. 2). For metallic materials it was shown^{87,95} that the spatial dispersion can play the same role as the residual relaxation by making the Casimir entropy equal to zero at zero temperature. It was also shown that with account of screening effects the Nernst theorem is satisfied for dielectrics whose conductivity vanishes with temperature exponentially fast due to the vanishing concentration of charge carriers.^{91,92} There are, however, dielectric materials, such as dielectric-type semiconductors, dielectrics with ionic conductivity and dielectric-type doped semiconductors, for which the concentration of charge carriers does not vanish with T whereas the conductivity goes to zero due to the vanishing mobility of charge carriers. For these dielectric materials the problem of violation of the Nernst heat theorem for the Casimir entropy remains unresolved.⁹⁴

Thus, although a consideration of the effects of spatial dispersion in the anomalous skin effect and screening effects leads to some encouraging results concerning a discrepancy of theoretical predictions of the Lifshitz theory with thermodynamics and experiment, it does not solve the problem of thermal Casimir force.

5. Could an Alternative Nonlocal Response to Evanescent Waves Solve the Problem?

The spatially nonlocal dielectric functions discussed in Sec. 4.3 describe the anomalous skin effect and screening effects observed in the propagating electromagnetic waves of rather high frequency and quasistatic fields, respectively. These functions were derived under the conditions $\omega \ll \omega_p$ and $k \ll k_F$ where k_F is the Fermi wave number.⁸⁹ As mentioned in Sec. 4.3, the respective transverse response functions are rather close to the local ones measured in the optical experiments performed in the area of propagating waves whereas the longitudinal ones deviate significantly from the local results.

It should be particularly emphasized that the longitudinal response function $\varepsilon^L(\omega, \mathbf{k})$ can be found not only from optical measurements but from experiments on measuring the energy loss and momentum transfer of high-energy electrons which belong to the beam passing through a thin metallic film.⁹⁶ As a result, from a fundamental standpoint, an experimental information about ε^L is available in both areas of the propagating and evanescent waves. There is, however, no experimental evidence about ε^{Tr} in the area of evanescent waves. Because of this, it might be unjustified to extrapolate the dielectric permittivities ε^{Tr} suitable for theoretical description of the anomalous skin effect or screening effects to the area of evanescent

waves and substitute them to the Lifshitz formula (2) in the frequency interval $0 \leq \omega \leq ck_{\perp}$.

Below we consider the phenomenological nonlocal response functions which do not aim to describe the anomalous skin effect or screening effects in real fields but provide some alternative in the area of evanescent waves off the mass shell which could provide a solution to the problem of thermal Casimir force. We begin with the representation of reflection coefficients applicable in the presence of spatial dispersion.

5.1. Reflection coefficients in the approximation of specular reflection

It is well known that the reflection coefficients on the boundary plane $\mathbf{r}_{\perp} = (x, y)$ of a material plate (the z axis is perpendicular to it) can be expressed in terms of the surface impedances defined as⁹⁶

$$Z_{\text{TM}}(\omega, k_{\perp}) = \frac{E_x(+0; \omega, k_{\perp})}{H_y(+0; \omega, k_{\perp})}, \quad Z_{\text{TE}}(\omega, k_{\perp}) = -\frac{E_y(+0; \omega, k_{\perp})}{H_x(+0; \omega, k_{\perp})}, \quad (13)$$

where all fields have the form

$$\mathbf{F}(t, \mathbf{r}) = \mathbf{F}(z; \omega, k_{\perp}) e^{-i\omega t + i\mathbf{k}_{\perp} \mathbf{r}_{\perp}}. \quad (14)$$

Using (13), the reflection coefficients are given by⁹⁶

$$r_{\text{TM}}(\omega, k_{\perp}) = \frac{cq + i\omega Z_{\text{TM}}(\omega, k_{\perp})}{cq - i\omega Z_{\text{TM}}(\omega, k_{\perp})}, \quad r_{\text{TE}}(\omega, k_{\perp}) = \frac{cq Z_{\text{TE}}(\omega, k_{\perp}) + i\omega}{cq Z_{\text{TE}}(\omega, k_{\perp}) - i\omega}. \quad (15)$$

If the plate material possesses only the temporal dispersion, the impedances (13) are equal to⁹⁷

$$Z_{\text{TM}}(\omega, k_{\perp}) = \frac{ick(\omega, k_{\perp})}{\omega\varepsilon(\omega)}, \quad Z_{\text{TE}}(\omega, k_{\perp}) = -\frac{i\omega\mu(\omega)}{ck(\omega, k_{\perp})}, \quad (16)$$

where $k(\omega, k_{\perp})$ is defined in (4), and (15) reduces to the standard Fresnel reflection coefficients (3).

If the plate material possesses the spatial dispersion, the expressions for surface impedances can be derived in the approximation of specular reflection (see Sec. 4.3). They take the following form:

$$\begin{aligned} Z_{\text{TM}}(\omega, k_{\perp}) &= \frac{i\omega c\mu(\omega)}{\pi} \int_{-\infty}^{\infty} \frac{dk_3}{\mathbf{k}^2} \left[\frac{k_{\perp}^2}{\varepsilon^{\text{L}}(\omega, \mathbf{k})\mu(\omega)\omega^2} + \frac{k_3^2}{\varepsilon^{\text{Tr}}(\omega, \mathbf{k})\mu(\omega)\omega^2 - c^2\mathbf{k}^2} \right], \\ Z_{\text{TE}}(\omega, k_{\perp}) &= \frac{i\omega c\mu(\omega)}{\pi} \int_{-\infty}^{\infty} \frac{dk_3}{\varepsilon^{\text{Tr}}(\omega, \mathbf{k})\mu(\omega)\omega^2 - c^2\mathbf{k}^2}, \end{aligned} \quad (17)$$

where $\mathbf{k} = (k_1, k_2, k_3)$. For nonmagnetic materials ($\mu = 1$) the expressions (17) have long been derived by different methods.^{89,98} The generalization for the case of magnetic materials was made very recently.⁹⁹

By putting $\omega = i\xi_l$ in (15) and (17), one can calculate the Casimir pressure between the plates with account of spatial dispersion using the Lifshitz formula (5).

This was made, for instance, for the nonmagnetic metal plates with account of the anomalous skin effect⁸⁶ but the results obtained were almost the same as are given by the standard Drude model (see Sec. 4.3).

5.2. An alternative response to the evanescent waves

Taking into account that an application of the standard spatially nonlocal response functions does not solve the problem of the thermal Casimir force, it was suggested^{65,66} that a model which describes well the response of metal to electromagnetic field on the mass shell may fail in describing the response to quantum fluctuations which are off the mass shell.

Following this line of attack, the spatially nonlocal Drude-like response functions were introduced¹⁰⁰

$$\begin{aligned}\varepsilon^{\text{Tr}}(\omega, k_{\perp}) &= 1 - \frac{\omega_p^2}{\omega[\omega + i\gamma(T)]} \left(1 + i \frac{v^{\text{Tr}} k_{\perp}}{\omega}\right), \\ \varepsilon^{\text{L}}(\omega, k_{\perp}) &= 1 - \frac{\omega_p^2}{\omega[\omega + i\gamma(T)]} \left(1 + i \frac{v^{\text{L}} k_{\perp}}{\omega}\right)^{-1},\end{aligned}\quad (18)$$

where v^{Tr} and v^{L} are the constants having a dimension of velocity which are of the order of Fermi velocity $v_{\text{F}} \sim 0.01c$.

The characteristic feature of the dielectric functions (18) is that for the electromagnetic waves on the mass shell in vacuum satisfying the condition $\omega > ck_{\perp}$ (i.e., for the propagating waves) they nearly coincide with the Drude dielectric permittivity (7) because

$$\frac{v^{\text{Tr,L}} k_{\perp}}{\omega} \sim \frac{v_{\text{F}}}{c} \frac{ck_{\perp}}{\omega} < \frac{v_{\text{F}}}{c} \ll 1. \quad (19)$$

Thus, the functions (18) take into account the relaxation properties of conduction electrons as does the Drude model. However, in the frequency region $0 \leq \omega \leq ck_{\perp}$ (i.e., for the evanescent waves) these functions can significantly depart from the Drude model leading to some new results in the theoretical description of physical effects caused by the electromagnetic fluctuations off the mass shell (an importance of the frequency region $\omega \ll kc$ for resolution of the problem of thermal Casimir force was also discussed using the hydrodynamic approximation for the response function¹⁰¹).

Computations of the effective Casimir pressure and the gradient of the Casimir force were made for Au-coated surfaces of a sphere and a plate in high precision experiments performed by means of a micromechanical torsional oscillator⁴⁵⁻⁴⁸ and an atomic force microscope⁶³⁻⁶⁶ using the optical data of Au and Eqs. (5), (12), (15), (17), and (18). For $v^{\text{Tr}} = v^{\text{L}} = 7v_{\text{F,Au}}$, the results obtained^{100,102} turned out to be in as good agreement with the measurement data as was reached earlier by using the nondissipative plasma model (8) (see Sec. 3).

Similar computations were performed⁹⁹ in the configuration of experiment^{68,69} on measuring the gradient of the Casimir force between the sphere and plate surfaces

coated with a magnetic metal Ni. The computational results taking dissipation into account by the dielectric functions (18) were found in a good agreement with the measurement data under the conditions $v^{\text{Tr}} = v^{\text{L}} = 7v_{\text{F,Ni}}$.

It is significant that both for Au and Ni test bodies only the first condition $v^{\text{Tr}} = 7v_{\text{F,Au(Ni)}}$ is necessary for reaching good agreement with the measurement data. As to the second parameter, v^{L} , it could vary in the interval from 0 to $10v_{\text{F}}$ with no impact on the measure of agreement between experiment and theory. This means that, unlike the case of nonlocal effects occurring in the propagating waves, in the off-the-mass-shell fields of quantum fluctuations the proper description of a dielectric response may demand significant departure of the transverse permittivity from its local form.

It was shown¹⁰³ that the Casimir entropy calculated using the Drude-like dielectric functions (18) satisfies the Nernst heat theorem, i.e., goes to zero with vanishing temperature for the perfect crystal lattices and also for lattices with impurities. We recall that the Casimir entropy calculated using the standard Drude model (7) violates the Nernst heat theorem for metals with perfect crystal lattices (see Sec. 2.1). In the literature,^{104,105} this violation was explained by an initiation of the correlated glassy state which is out of thermal equilibrium. Furthermore, according to the results obtained,¹⁰⁰ the permittivities (18) satisfy the Kramers-Kronig relations derived for analytic functions with poles of the first and second order at zero frequency and do not lead to contradictions with the measurement data of optical experiments exploiting the propagating waves.

It is pertinent to stress that the Drude-like response functions (18) depend only on k_{\perp} . Taking into account, however, that the fictitious space discussed in Sec. 4.3 is a 3D homogeneous manifold, it would be more general to consider nonlocal functions depending on all the wave vector components. Based on this, the simplest generalization of (18) was suggested¹⁰⁶

$$\begin{aligned}\varepsilon^{\text{Tr}}(\omega, k) &= 1 - \frac{\omega_p^2}{\omega[\omega + i\gamma(T)]} \left(1 + i\frac{v^{\text{Tr}}k}{\omega}\right), \\ \varepsilon^{\text{L}}(\omega, k) &= 1 - \frac{\omega_p^2}{\omega[\omega + i\gamma(T)]} \left(1 + i\frac{v^{\text{L}}k}{\omega}\right)^{-1},\end{aligned}\quad (20)$$

where $k = |\mathbf{k}| = (k_{\perp}^2 + k_3^2)^{1/2}$.

Computations of the gradient of the Casimir force using the optical data and Eqs. (5), (12), (15), (17), and (20) were performed in the configurations of experiments exploiting the Au-coated^{65,66} and Ni-coated^{68,69} surfaces of a sphere and a plate at $T = 300$ K with $v^{\text{Tr}} = v^{\text{L}} = 3v_{\text{F,Au(Ni)}}/2$. The computational results for the Au-coated test bodies are shown in Fig. 8 (left) by the top band and for the Ni-coated ones in Fig. 8 (right) by the bottom band as the functions of separation.¹⁰⁶ The bottom band in Fig. 8 (left) and the top band in Fig. 8 (right) are computed using the Drude model extrapolation of the optical data. The experimental data are shown as crosses where the measurement errors were found at the 67% confidence level.

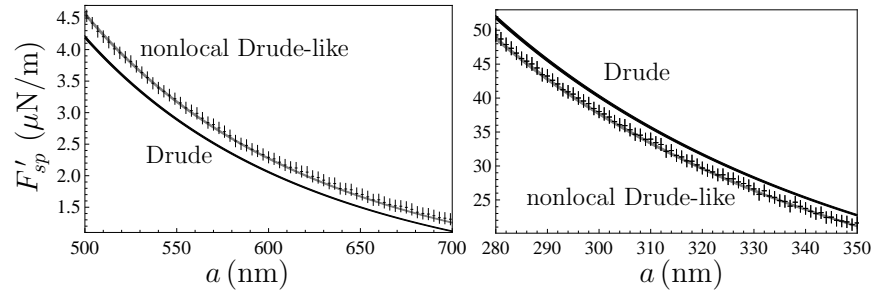


Fig. 8. The gradient of the Casimir force between an Au-coated sphere and an Au-coated plate computed at $T = 300$ K using either the Drude or nonlocal Drude-like extrapolations of the optical data is shown as a function of separation by the bottom and top bands, respectively (left). For the Ni-coated surfaces of a sphere and a plate, the force gradient computed at $T = 300$ K using either the nonlocal Drude-like or Drude extrapolations is shown by the bottom and top bands, respectively (right). In both cases the measurement data are shown as crosses.

As is seen in Fig. 8, the computational results using the Drude-like response functions (20) are in a good agreement with the measurement data. The theoretical predictions using the Drude model are experimentally excluded. By comparing Fig. 8 (left) with Fig. 5 (right) and Fig. 8 (right) with Fig. 6 (right) one can conclude that the theoretical predictions of the Lifshitz theory using the nonlocal permittivities (20) taking into account the dissipation of free charge carriers are indistinguishable from the predictions of the same theory made by using the dissipationless plasma model. For the experiment employing dissimilar Au- and Ni-coated test bodies⁶⁷ an employment of the nonlocal permittivities (20) with $v^{\text{Tr}} = v^{\text{L}} = 3v_{\text{F,Au(Ni)}}/2$ results in the theoretical band coinciding with that in Fig. 6 (left) which is in agreement with the measurement data.

Note that except of entirely theoretical advantage of the permittivities (20) compared to (18), they also lead to by a factor of 4.7 smaller values of the constants v^{Tr} and v^{L} providing an agreement between experiment and theory in measuring the Casimir force. This makes even smaller any corrections arising from using (20) in place of the standard Drude model (7) in interpretation of optical experiments performed in the area of propagating waves. It is important also that the value of constant v^{L} in (20), as well as in (18), can vary in the interval from 0 to $10v_{\text{F,Au(Ni)}}$ with no impact on the measure of agreement between the theoretical Casimir forces and the measurement data. This means that the major role in this agreement is played by the Drude-like dielectric function $\varepsilon^{\text{Tr}}(\omega, \mathbf{k})$. As to $\varepsilon^{\text{L}}(\omega, \mathbf{k})$, it can be replaced even with the standard Drude model (7).

6. Conclusions and Outlook

In the foregoing, we have considered the problem of thermal Casimir force actively discussed in the literature for the last twenty years. This problem lies in the fact that theoretical predictions of the fundamental Lifshitz theory obtained using the universally accepted dielectric functions are inconsistent with the measurement data

of high precision experiments and in some cases (idealized model of metals with perfect crystal lattices, dielectrics with account of electric conductivity at nonzero temperature) are found to be in conflict with the Nernst heat theorem.

After presenting the results of numerous experiments on measuring the thermal Casimir force performed by means of a micromechanical torsional oscillator and an atomic force microscope, we have outlined extensive studies of the problem directed to its resolution. These include an investigation of the validity and application regions of various approximate methods, including the PFA and the additive approach to surface roughness, and an analysis of the role of possible unaccounted effects, such as surface patches and sample-to-sample variation of the optical data. Particular attention has been given to a generalization of the Lifshitz theory with account of spatial dispersion and screening effects. It is shown that although the use of nonlocal response functions derived in the literature for theoretical description of the anomalous skin effect and screening effects leads to some encouraging results, the problem of disagreement between experiment and theory remained unresolved.

Finally, the method of attack was considered which attracts special attention to the fact that the transverse response function to the evanescent waves cannot be determined experimentally and its correct form may be unobtainable by the analytic continuation of familiar nonlocal permittivities describing, e.g., the anomalous skin effect. The recently suggested phenomenological nonlocal Drude-like response functions are discussed which take proper account of the dissipation of conduction electrons and simultaneously bring the Lifshitz theory in agreement with all high precision experiments on measuring the Casimir force between metallic surfaces and with the Nernst heat theorem.

In the future, it would be desirable to develop a complete description of the dielectric response of both metallic and dielectric materials based on first principles of quantum electrodynamics at nonzero temperature. This could be attained by deriving the polarization tensor of electronic plasmas in dielectrics and metals like this is already done for graphene in the framework of the Dirac model.^{107–109} The first step in this direction is already made by finding the polarization tensor of the three-dimensional Dirac material.¹¹⁰ One may hope that the fundamental derivation of response functions will make it possible not only to obtain familiar results describing the anomalous skin effect and screening effects as the special cases in the area of propagating waves, but also justify the phenomenological permittivities proposed in Sec. 5 as the asymptotic results in the area of evanescent waves. In our opinion, this is a plausible way toward final resolution of the problem of thermal Casimir force.

Acknowledgments

This work was partially supported by the Peter the Great Saint Petersburg Polytechnic University in the framework of the Russian state assignment for basic research (project No. FSEG-2020-0024). This paper has been supported by the Kazan

Federal University Strategic Academic Leadership Program.

References

1. H. B. G. Casimir, *Proc. Kon. Ned. Akad. Wet. B* **51**, 793 (1948).
2. M. Fierz, *Helv. Phys. Acta* **33**, 855 (1960).
3. J. Mehra, *Physica* **37**, 145 (1967).
4. L. S. Braun and G. J. Maclay, *Phys. Rev.* **184**, 1272 (1969).
5. H. Mitter and D. Robaschik, *Eur. Phys. J. B* **13**, 335 (2000).
6. E. M. Lifshitz, *Zh. Eksp. Teor. Fiz.* **29**, 94 (1955) [*Sov. Phys. JETP* **2**, 73 (1956)].
7. P. Richmond and B. W. Ninham, *J. Phys. C: Solid St. Phys.* **4**, 1988 (1971).
8. N. G. Van Kampen, B. R. A. Nijboer and K. Schram, *Phys. Lett. A* **26**, 307 (1968).
9. B. W. Ninham, V. A. Parsegian and G. H. Weiss, *J. Stat. Phys.* **2**, 323 (1970).
10. K. Schram, *Phys. Lett. A* **43**, 282 (1973).
11. Yu. S. Barash and V. L. Ginzburg, *Usp. Fiz. Nauk* **116**, 5 (1975) [*Sov. Phys. Usp.* **18**, 305 (1975)].
12. J. Schwinger, L. L. DeRaad and K. A. Milton, *Ann. Phys. (N.Y.)* **115**, 1 (1978).
13. K. A. Milton, *Ann. Phys. (N.Y.)* **150**, 432 (1983).
14. K. A. Milton, *The Casimir Effect: Physical Manifestations of Zero-Point Energy* (World Scientific, Singapore, 2001).
15. L. H. Ford, *Phys. Rev. D* **11**, 3370 (1975).
16. S. G. Mamaev, V. M. Mostepanenko and A. A. Starobinsky, *Zh. Eksp. Teor. Fiz.* **70**, 1577 (1976) [*Sov. Phys. JETP* **43**, 823 (1976)].
17. M. Bordag, G. L. Klimchitskaya, U. Mohideen and V. M. Mostepanenko, *Advances in the Casimir Effect* (Oxford University Press, Oxford, 2015).
18. M. Boström and Bo E. Sernelius, *Phys. Rev. Lett.* **84**, 4757 (2000).
19. *Handbook of Optical Constants of Solids*, edited by E. D. Palik (Academic Press, New York, 1985).
20. L. D. Landau, E. M. Lifshitz and L. P. Pitaevskii, *Electrodynamics of Continuous Media* (Pergamon, Oxford, 1984).
21. N. W. Ashcroft and N. D. Mermin, *Solid State Physics* (Saunders College, Philadelphia, 1976).
22. A. Lambrecht and S. Reynaud, *Eur. Phys. J. D* **8**, 309 (2000).
23. C. Genet, A. Lambrecht and S. Reynaud, *Phys. Rev. A* **62**, 012110 (2000).
24. M. Bordag, B. Geyer, G. L. Klimchitskaya and V. M. Mostepanenko, *Phys. Rev. Lett.* **85**, 503 (2000).
25. V. B. Bezerra, G. L. Klimchitskaya, V. M. Mostepanenko and C. Romero, *Phys. Rev. A* **69**, 022119 (2004).
26. M. Bordag and I. Pirozhenko, *Phys. Rev. D* **82**, 125016 (2010).
27. G. L. Klimchitskaya and V. M. Mostepanenko, *Phys. Rev. A* **95**, 012130 (2017).
28. G. L. Klimchitskaya and C. C. Korikov, *Phys. Rev. A* **91**, 032119 (2015).
29. S. Boström and Bo E. Sernelius, *Physica A* **339**, 53 (2004).
30. I. Brevik, J. B. Aarseth, J. S. Høye and K. A. Milton, *Phys. Rev. E* **71**, 056101 (2005).
31. J. S. Høye, I. Brevik, S. A. Ellingsen and J. B. Aarseth, *Phys. Rev. E* **75**, 051127 (2007).
32. B. V. Derjaguin, I. I. Abrikosova and E. M. Lifshitz, *Quat. Rev.* **10**, 295 (1956).
33. D. Tabor and R. H. S. Winterton, *Nature* **219**, 1120 (1968).
34. J. N. Israelachvili and D. Tabor, *Proc. Roy. Soc. Lond. A* **331**, 19 (1972).
35. J. N. Israelachvili, *Intermolecular and Surface Forces* (Academic Press, San Diego,

- 1992).
36. J. M. Obrecht, R. J. Wild, M. Antezza, L. P. Pitaevskii, S. Stringari and E. A. Cornell, *Phys. Rev. Lett.* **98**, 063201 (2007).
 37. B. Geyer, G. L. Klimchitskaya and V. M. Mostepanenko, *Phys. Rev. D* **72**, 085009, (2005).
 38. G. L. Klimchitskaya, U. Mohideen and V. M. Mostepanenko, *J. Phys. A: Math. Theor.* **41**, 432001 (2008).
 39. G. L. Klimchitskaya and C. C. Korikov, *J. Phys.: Condens. Matter* **27**, 214007 (2015).
 40. G. L. Klimchitskaya and V. M. Mostepanenko, *J. Phys.: Condens. Matter* **29**, 275701 (2017).
 41. G. L. Klimchitskaya, E. V. Blagov and V. M. Mostepanenko, *Int. J. Mod. Phys. A* **24**, 1777, (2009).
 42. C. C. Korikov and V. M. Mostepanenko, *Mod. Phys. Lett. A* **35**, 2040010 (2020).
 43. S. A. Ellingsen, I. Brevik, J. S. Høye and K. A. Milton, *Phys. Rev. E* **78**, 021117 (2008).
 44. A. O. Sushkov, W. J. Kim, D. A. R. Dalvit and S. K. Lamoreaux, *Nat. Phys.* **7**, 230 (2011).
 45. R. S. Decca, E. Fischbach, G. L. Klimchitskaya, D. E. Krause, D. López and V. M. Mostepanenko, *Phys. Rev. D* **68**, 116003 (2003).
 46. R. S. Decca, D. López, E. Fischbach, G. L. Klimchitskaya, D. E. Krause and V. M. Mostepanenko, *Ann. Phys. (N.Y.)* **318**, 37 (2005).
 47. R. S. Decca, D. López, E. Fischbach, G. L. Klimchitskaya, D. E. Krause and V. M. Mostepanenko, *Phys. Rev. D* **75**, 077101 (2007).
 48. R. S. Decca, D. López, E. Fischbach, G. L. Klimchitskaya, D. E. Krause and V. M. Mostepanenko, *Eur. Phys. J. C* **51**, 963 (2007).
 49. M. Bordag, G. L. Klimchitskaya and V. M. Mostepanenko, *Int. J. Mod. Phys. A* **10**, 2661 (1995).
 50. G. L. Klimchitskaya, U. Mohideen and V. M. Mostepanenko, *Rev. Mod. Phys.* **81**, 1827 (2009).
 51. G. Bimonte, *Phys. Rev. Lett.* **112**, 240401 (2014).
 52. G. Bimonte, *Phys. Rev. B* **91**, 205443 (2015).
 53. G. Bimonte, D. López and R. S. Decca, *Phys. Rev. B* **93**, 184434 (2016).
 54. G. Bimonte, B. Spreng, P. A. Maia Neto, G.-L. Ingold, G. L. Klimchitskaya, V. M. Mostepanenko and R. S. Decca, *Universe* **7**, 93 (2021).
 55. M. Hartmann, G.-L. Ingold and P. A. Maia Neto, *Phys. Rev. Lett.* **119**, 043901 (2017).
 56. B. Spreng, M. Hartmann, V. Henning, P. A. Maia Neto and G.-L. Ingold, *Phys. Rev. A* **97**, 062504 (2018).
 57. M. Hartmann, G.-L. Ingold and P. A. Maia Neto, *Phys. Scr.* **93**, 114003 (2018).
 58. V. Henning, B. Spreng, M. Hartmann, G.-L. Ingold and P. A. Maia Neto, *J. Opt. Soc. Amer. B* **36**, C77 (2019).
 59. C. D. Fosco, F. C. Lombardo and F. D. Mazzitelli, *Phys. Rev. D* **84**, 105031 (2011).
 60. G. Bimonte, T. Emig, R. L. Jaffe and M. Kardar, *Europhys. Lett.* **97**, 50001 (2012).
 61. G. Bimonte, T. Emig and M. Kardar, *Appl. Phys. Lett.* **100**, 074110 (2012).
 62. G. Bimonte, *Europhys. Lett.* **118**, 20002 (2017).
 63. C.-C. Chang, A. A. Banishev, R. Castillo-Garza, G. L. Klimchitskaya, V. M. Mostepanenko and U. Mohideen, *Phys. Rev. B* **85**, 165443 (2012).
 64. J. Xu, G. L. Klimchitskaya, V. M. Mostepanenko and U. Mohideen, *Phys. Rev. A* **97**, 032501 (2018).
 65. M. Liu, J. Xu, G. L. Klimchitskaya, V. M. Mostepanenko and U. Mohideen, *Phys.*

- Rev. B* **100**, 081406(R) (2019).
66. M. Liu, J. Xu, G. L. Klimchitskaya, V. M. Mostepanenko and U. Mohideen, *Phys. Rev. A* **100**, 052511 (2019).
 67. A. A. Banishev, C.-C. Chang, G. L. Klimchitskaya, V. M. Mostepanenko and U. Mohideen, *Phys. Rev. B* **85**, 195422 (2012).
 68. A. A. Banishev, G. L. Klimchitskaya, V. M. Mostepanenko and U. Mohideen, *Phys. Rev. Lett.* **110**, 137401 (2013).
 69. A. A. Banishev, G. L. Klimchitskaya, V. M. Mostepanenko and U. Mohideen, *Phys. Rev. B* **88**, 155410 (2013).
 70. F. Chen, G. L. Klimchitskaya, V. M. Mostepanenko and U. Mohideen, *Optics Express* **15**, 4823 (2007).
 71. F. Chen, G. L. Klimchitskaya, V. M. Mostepanenko and U. Mohideen, *Phys. Rev. B* **76**, 035338 (2007).
 72. C.-C. Chang, A. A. Banishev, G. L. Klimchitskaya, V. M. Mostepanenko and U. Mohideen, *Phys. Rev. Lett.* **107**, 090403 (2011).
 73. A. A. Banishev, C.-C. Chang, R. Castillo-Garza, G. L. Klimchitskaya, V. M. Mostepanenko and U. Mohideen, *Phys. Rev. B* **85**, 045436 (2012).
 74. G. L. Klimchitskaya and V. M. Mostepanenko, *J. Phys. A: Math. Theor.* **41**, 312002 (2008).
 75. P. A. Maia Neto, A. Lambrecht and S. Reynaud, *Phys. Rev. A* **78**, 012115 (2008).
 76. A. Canaguier-Durand, P. A. Maia Neto, I. Cavero-Pelaez, A. Lambrecht and S. Reynaud, *Phys. Rev. Lett.* **102**, 230404 (2009).
 77. P. J. van Zwol, G. Palasantzas and J. Th. M. De Hosson, *Phys. Rev. B* **77**, 075412 (2008).
 78. W. Broer, G. Palasantzas, J. Knoester and V. B. Svetovoy, *Phys. Rev. B* **85**, 155410 (2012).
 79. C. Genet, A. Lambrecht, P. A. Maia Neto and S. Reynaud, *Europhys. Lett.* **62**, 484 (2003).
 80. P. A. Maia Neto, A. Lambrecht and S. Reynaud, *Phys. Rev. A* **72**, 012115 (2005).
 81. C. C. Speake and C. Trenkel, *Phys. Rev. Lett.* **90**, 160403 (2003).
 82. R. O. Behunin, F. Intravaia, D. A. R. Dalvit, P. A. Maia Neto and S. Reynaud, *Phys. Rev. A* **85**, 012504 (2012).
 83. R. O. Behunin, D. A. R. Dalvit, R. S. Decca, C. Genet, I. W. Jung, A. Lambrecht, A. Liscio, D. López, S. Reynaud, G. Schnoering, G. Voisin and Y. Zeng, *Phys. Rev. A* **90**, 062115 (2014).
 84. I. Pirozhenko, A. Lambrecht and V. B. Svetovoy, *New J. Phys.* **8**, 238 (2006).
 85. V. B. Svetovoy, P. J. van Zwol, G. Palasantzas and J. Th. M. De Hosson, *Phys. Rev. B* **77**, 035439 (2008).
 86. R. Esquivel and V. B. Svetovoy, *Phys. Rev. A* **69**, 062102 (2004).
 87. Bo E. Sernelius, *Phys. Rev. B* **71**, 235114 (2005).
 88. J.-N. Chazalviel, *Coulomb Screening of Mobile Charges: Applications to Material Science, Chemistry and Biology* (Birkhauser, Boston, 1999).
 89. K. L. Kliewer and R. Fuchs, *Phys. Rev.* **172**, 607 (1968).
 90. N. D. Mermin, *Phys. Rev. B* **1**, 2362 (1970).
 91. L. P. Pitaevskii, *Phys. Rev. Lett.* **101**, 163202 (2008).
 92. V. B. Svetovoy, *Phys. Rev. Lett.* **101**, 163603 (2008).
 93. D. A. R. Dalvit and S. K. Lamoreaux, *Phys. Rev. Lett.* **101**, 163203 (2008).
 94. V. M. Mostepanenko, R. S. Decca, E. Fischbach, B. Geyer, G. L. Klimchitskaya, D. E. Krause, D. López, U. Mohideen, *Int. J. Mod. Phys. A* **24**, 1721 (2009).
 95. V. B. Svetovoy and R. Esquivel, *Phys. Rev. E* **72**, 036113 (2005).

26 *G. L. Klimchitskaya & V. M. Mostepanenko*

96. M. Dressel and G. Grüner, *Electrodynamics of Solids: Optical Properties of Electrons in Metals* (Cambridge University Press, Cambridge, 2003).
97. R. Esquivel, C. Villarreal and W. L. Mochán, *Phys. Rev. A* **68**, 052103 (2003); **71**, 029904(E) (2005).
98. V. P. Silin and E. P. Fetisov, *Zh. Eksp. Teor. Fiz.* **41**, 159 (1961) [*Sov. Phys. JETP* **14**, 115 (1962)].
99. G. L. Klimchitskaya and V. M. Mostepanenko, *Phys. Rev. D* **104**, 085001 (2021).
100. G. L. Klimchitskaya and V. M. Mostepanenko, *Eur. Phys. J. C* **80**, 900 (2020).
101. M. Hannemann, G. Wegner and C. Henkel, *Universe* **7**, 108 (2021).
102. V. M. Mostepanenko, *Universe* **7**, 84 (2021).
103. G. L. Klimchitskaya and V. M. Mostepanenko, *Phys. Rev. D* **103**, 096007 (2021).
104. F. Intravaia and C. Henkel, *Phys. Rev. Lett.* **103**, 130405 (2009).
105. F. Intravaia, S. Ellingsen and C. Henkel, *Phys. Rev. A* **82**, 032504 (2010).
106. G. L. Klimchitskaya and V. M. Mostepanenko, *Phys. Rev. A* **105**, 012805 (2022).
107. I. V. Fialkovsky, V. N. Marachevsky and D. V. Vassilevich, *Phys. Rev. B* **84**, 035446 (2011).
108. M. Bordag, G. L. Klimchitskaya, V. M. Mostepanenko and V. M. Petrov, *Phys. Rev. D* **91**, 045037 (2015); **93**, 089907(E) (2016).
109. M. Bordag, I. Fialkovskiy and D. Vassilevich, *Phys. Rev. B* **93**, 075414 (2016); **95**, 119905(E) (2017).
110. M. Bordag, I. V. Fialkovsky, N. Khusnutdinov and D. V. Vassilevich, *Phys. Rev. B* **104**, 195431 (2021).